Chapter

Tetradentate Platinum(II) Emitters: Design Strategies, Photophysics, and OLED Applications

Huiyang Li, Tsz-Lung Lam, Liangliang Yan, Lei Dai, Byoungki Choi, Yong-Suk Cho, Yoonhyun Kwak and Chi-Ming Che

Abstract

This chapter provides an overview of tetradentate platinum(II) emitters as a promising class of metal-organic phosphorescent dopants for organic light-emitting diodes (OLEDs). Tetradentate platinum(II) emitters showing blue, green, and red light emissions, which are essential for full color displays as well as white light emission, are reviewed and discussed in the context of molecular design and photophysical and electroluminescent properties. Emphasis is placed on the molecular structures, the nature of emissive excited states [including ligand-centered (LC), intra-ligand charge transfer (ILCT), metal-to-ligand charge transfer (MLCT), and excimeric and oligomeric metal-metal-to-ligand charge transfer (MMLCT)], the intermolecular interactions impacting photophysical attributes (e.g., emission energies, quantum yields, and decay times), and OLED device performances.

Keywords: organic light-emitting diodes, metal complexes, platinum, phosphorescence, high efficiency, operational lifetime

1. Introduction

Organic light-emitting diodes (OLEDs) are solid-state devices based on organic films sandwiched between two electrodes that convert electricity to luminous energy. Since the pioneering work of electroluminescence (EL) in 1987 [1], OLEDs have been attracting considerable attention because of their light weight, low driving voltage, low power consumption, fast response speed, and high frame rate for displays, making them suitable for various applications [2–5], e.g., wearable devices, virtual reality (VR), smart homes and cities, and imaging and sensing applications. Currently, products with OLED displays are found in several fields, ranging from micro-displays to TV applications, and notably in smartphones and personal computers.

Figure 1 shows the typical structure of an OLED device, including a number of thin layers, which individually facilitate charge transfer or light emission [6–9]. During operation, when a suitable voltage is applied, electrons are injected into

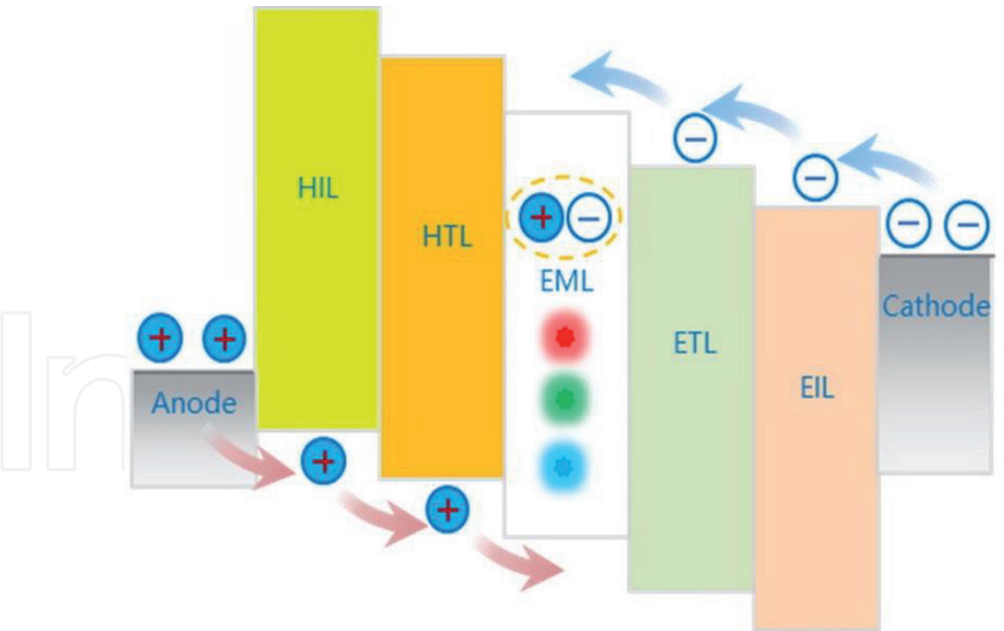

Figure 1.
Structure of an OLED device.

the electron transporting layer (ETL) from the metal cathode, which generally has a low work function (e.g., Al or Ag). To facilitate this process, a 0.5- to 1.0-nm thick electron injection layer (EIL) of LiF or CsF is usually deposited between the cathode and the ETL. Electrons migrate by hopping toward the anode. Meanwhile, holes are injected from the anode, which usually consists of a metal oxide mixture of SnO_2 (10%) and In_2O_3 (90%), namely, indium tin oxide (ITO). Following the anode, a hole injection layer (HIL) and a hole transporting layer (HTL) are typically required to promote hole transfer into the emission layer (EML), which includes the host matrix and dopant. Ideally, the recombination of electrons and holes takes place in the EML, subsequently populating the excited states that generate light emission. Obviously, the electron current must be well balanced with the hole current to avoid ohmic loss, which can be minimized by employing a hole blocking layer (HBL) between the ETL and EML and/or an electron blocking layer (EBL) between the HTL and EML. These blocking layers prevent the holes and electrons from leaving the EML without recombination. In addition, each layer requires materials with suitable highest occupied molecular orbital (HOMO) and lowest unoccupied molecular orbital (LUMO) energy levels. The development of auxiliary OLED materials (e.g., materials for the HTL, ETL, HBL, and EBL) has been the subject of previous reviews and is not discussed in this chapter [10–13].

As described above, the electrons and holes recombine and form neutral excitons in the EML. According to spin statistics, the recombination will populate singlet and triplet excited states in a ratio of 1:3, meaning that 75% of the electrically excited states are triplet states [14]. Pure organic molecules usually do not show spin-forbidden triplet emission (i.e., phosphorescence) at room temperature [15, 16], and normally only the singlet exciton is emissive, resulting in limited quantum efficiency, which presents a challenge for improving the efficiency of OLED devices. In 1998, the first successful applications of organometallic complexes as emissive dopant material in electroluminescent devices to generate phosphorescence were independently reported by Ma and Che [17] as well as Thompson and Forrest [18]. This revolutionary appraoch offers a viable means for the maximum use of electically generated excitons for electroluminescence and allowed a substantial leap forward in OLED performance. Since then, there has been increasing

interest in the design and synthesis of new phosphorescent metal complexes, particularly those of Ru(II), Ir(III), and Pt(II), as OLED dopants [19–22].

2. Platinum(II) complexes as phosphorescent OLED dopants

Phosphorescent metal complexes remain mainstream OLED emitters, because relative to pure organic fluorophores, they can more efficiently harvest excitons for light emission. Phosphorescent metal complexes typically possess a transition metal ion with a high atomic number, e.g., Ru(II), Ir(III), or Pt(II), that can induce strong spin-orbit coupling (SOC), giving rise to ultrafast intersystem crossing (ISC) from the singlet to triplet states and promoting spin-forbidden triplet radiative decay. This triplet harvesting mechanism theoretically enables complete utilization of the excitons generated by electron-hole recombination for light emission, leading to a much higher efficiency and luminance. Reasonable phosphorescent metal OLED emitters should exhibit the following traits: (i) high phosphorescent quantum yields (i.e., >70%) when doped in a solid matrix, (ii) tunable emission color covering the blue, green, and red spectral regions (essential for full color displays), and (iii) superior thermal, chemical, and electrochemical stabilities for vacuum deposition and operation. The plethora of literature examples demonstrated that phosphors based on Ir(III) and Pt(II) can meet these requirements and generally outperform other metal phosphors [20–22]. In the past two decades, extensive research efforts on OLED emitters have been devoted to the development of phosphorescent Ir(III) and Pt(II) complexes and to investigations of their photophysical, electrochemical, and electroluminescent characteristics.

Phosphorescent Pt(II) complexes are noted for their desirable photophysical properties; they have a square planar coordination geometry, are coordinatively unsaturated, and exhibit diverse highly emissive excited states, including ligand-centered (LC), intra-ligand charge transfer (ILCT), ligand-to-ligand charge transfer (LLCT), metal-to-ligand charge transfer (MLCT), and excimeric and oligomeric metal-metal-to-ligand charge transfer (MMLCT) states [21, 22]. Tailoring the emission attributes (i.e., energy, quantum yield, lifetime, and radiative and non-radiative decay rate constants) to suit specific OLED applications can be achieved by the rational design of ligands, which allows regulation of (i) the energy levels of the metal d orbitals, the π and π^* orbitals of the ligands, and subsequently the composition of the frontier molecular orbitals, excited-state dynamics, and the nature of the emissive excited state and (ii) the intermolecular interactions that can contribute to emission from an aggregated state and/or emission quenching. As is the case for all phosphorescent OLED emitters, engineering the emissive excited state of Pt(II) emitters with high metal character to keep the emission lifetime short is important, since saturation of electroluminescence, severe efficiency roll-off at high luminance, and poor operational stability could otherwise result.

The planar coordination geometry renders platinum(II) complexes susceptible to self-assembly in ground and/or excited states through intermolecular ligand π-π and/or Pt-Pt interactions. This intrinsic property usually leads to a considerable redshift in the absorption and emission energies attributed to the generation of the low-energy emissive MMLCT excited states with enhanced radiative decay rate constants [21, 22], which could be harnessed to provide unique access to long-range ordered luminescent supramolecular structures, non-doped NIR OLEDs, and single-doped white OLEDs (WOLEDs). Nevertheless, this aggregation behavior could be unfavorable for applications in RGB OLED panels, especially when the Pt(II) emitters are doped at high concentrations, due to the possible occurrence of aggregate emission, triplet-triplet annihilation (TTA) and aggregation-caused

quenching (ACQ). Therefore, the appropriate management of intermolecular interactions/aggregation by modulating the 3D morphology and electromagnetic properties of the complexes is crucial in the molecular design of Pt(II) emitters for specific OLED applications in order to achieve optimum device performances (i.e., high color purity, device efficiency, and long operational lifetime).

In the context of ligand architecture, the employment of tetradentate ligands in the design of platinum(II) emitters has clear advantages in terms of both chemical and thermal stabilities and luminescent efficiency compared to their bidentate and tridentate ligand counterparts. Tetradentate ligands provide a more stable scaffold for the coordination of platinum by offering the strong chelation effect, which could suppress ligand dissociation and demetalation. In addition, the rigid tetradentate ligand framework could largely restrict the excited-state metal-ligand structural distortion that in turn facilitates radiative deactivation of the emissive excited state, boosting the emission quantum yield of the Pt(II) emitter.

This chapter aims to provide an overview of mononuclear Pt(II) emitters containing tetradentate ligands reported in the literature. To keep the chapter to a reasonable size, we restrict our discussions to several selected classes of tetradentate platinum(II) emitters and apologize to the contributors to this field whose contributions are not mentioned herein.

3. Tetradentate platinum(II) emitters

3.1 Platinum(II) porphyrin complexes

The first photophysical studies of Pt(II) porphyrins were reported in the early 1970s and were triggered by the physicochemical relevance of metalloporphyrins such as chlorophyll, haem, and vitamin B12, which serve key biological functions [23]. This class of complexes is known for their high stability against heat, solvents, and extreme pH as a result of the strong coordination of Pt(II) ions in rigid porphyrin scaffolds. Pt(II) porphyrins exhibit intense absorptions in the visible region, and their electronic spectra are characterized by a Soret band at approximately 400 nm and two Q bands between 500 and 600 nm, which are attributed to porphyrin-centered $^1\pi$-π^* electronic transitions. The triplet formation yields for Pt(II) porphyrins were reported to be close to unity due to an ultrafast intersystem crossing process that occurs on a sub-ps time scale [24]. These complexes typically display strong saturated red to near infrared (NIR) phosphorescence, depending on the structures of macrocycles, with long decay times of tens of microseconds under anaerobic conditions because the emissive excited state is essentially ^{3}LC ($^3\pi$, π^*) in nature localized in the porphyrin ligand. For this reason, the emission properties can be rationally tuned by modifying the porphyrin ligands.

In 1998, Thompson and Forest reported the first use of a Pt(II) porphyrin complex, **Pt-1**, in electrophosphorescent devices (**Figure 2**) [18], which generated saturated red EL emission at 650 nm with a peak internal quantum efficiency (IQE) of 23%. Since then, the development of Pt(II) porphyrin complexes as phosphorescent emitters has attracted considerable interest [25–27].

Che et al. found that with the introduction of electron-deficient pentafluorophenyl rings at the meso positions of the porphyrin scaffold, **Pt-2** exhibited superior stability against oxidative degradation relative to that of the parental complex [Pt(TPP)] (TPP = 5,10,15,20-tetraphenylporphyrinato) (**Figure 2**) [28]. Saturated red (λ_{max} = 647 nm) porphyrin-centered phosphorescence with a long lifetime (τ_{em} = 60 μs) was observed for **Pt-2** in CH_2Cl_2 at room temperature. Saturated red OLED devices with different doping concentrations of **Pt-2** have

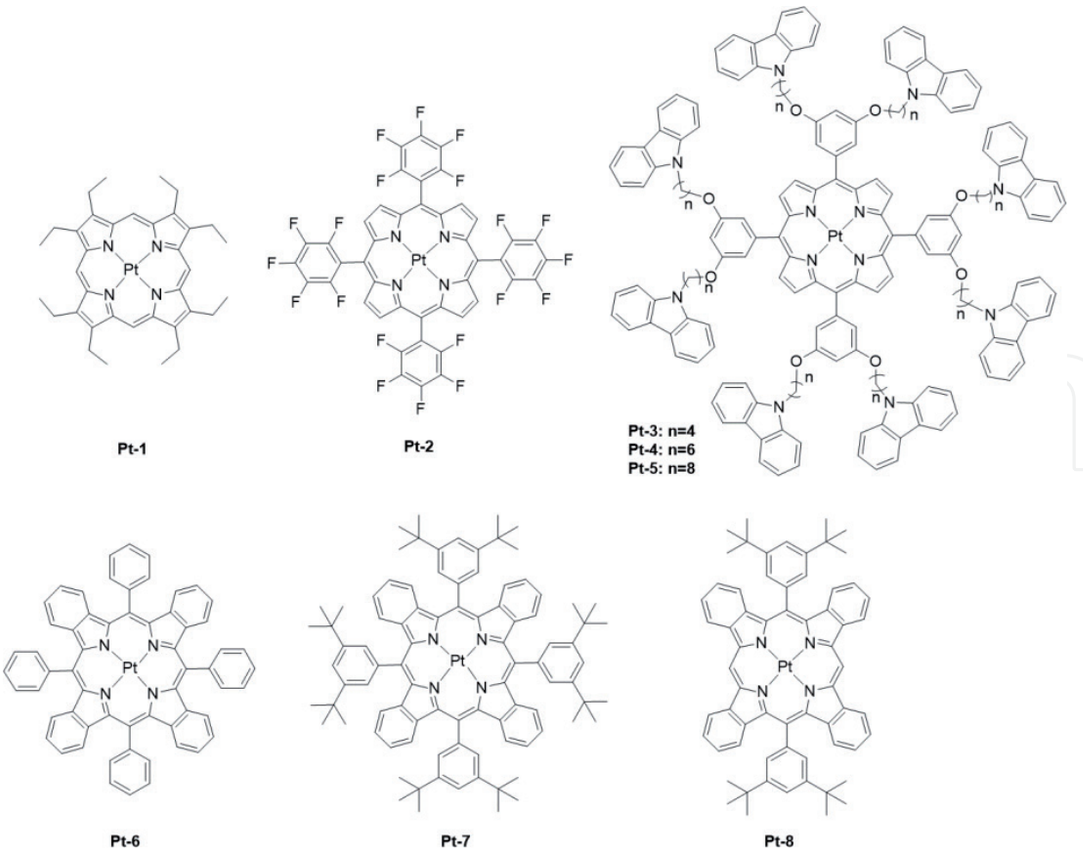

Figure 2.
*Chemical structures of platinum(II) porphyrin complexes **Pt-1–8**.*

been characterized. The EL spectra showed emission maxima at 655 nm, similar to that of the photoluminescent (PL) spectrum. At low driving voltages, emission from the host was not detected, indicating nearly complete energy transfer from the host. When a high voltage was applied, a blue emission from the host was observed, and its intensity increased with the driving voltage, which could be attributed to the saturation effect due to the long emission decay time of **Pt-2**. The efficiency increased until the dopant ratio reached 8% but decreased when the ratio was increased beyond 8%, which was rationalized by intermolecular quenching processes due to the high density of triplet excitons.

Wang and co-workers designed a group of platinum(II) porphyrin dendrimers (**Pt-3–5**) [29] with different alkyl chain lengths to adjust the distance between the Pt porphyrin core (the emissive center) and side carbazole groups (hole- and energy-transfer fragments) (**Figure 2**) and systematically investigated intra- and intermolecular energy-transfer mechanisms. In solution, both fluorescence at 357 nm from the carbazole moieties and phosphorescence at 660 nm from the Pt(II) porphyrin core were observed. The carbazole emission disappeared when doped in a solid matrix, indicating an efficient energy-transfer process. Intramolecular energy-transfer was facilitated by reducing the distance between the emitting core and the side carbazole groups. Solution-processed EL devices based on **Pt-3** were fabricated with a structure of [ITO/poly(styrenesulfonate)-doped poly(3,4-ethylenedioxythiophene)/**Pt-3**/2,9-dimethyl-4,7-diphenyl-1,10-phenanthroline (BCP)/tris-(8-hydroxyquinoline)aluminum (Alq_3)/Ca/Al] to evaluate the optoelectronic properties. Bright phosphorescence (600 cd/m^2) with emission maxima at 540, 590, 660, and 720 nm was observed. The strong vibronic emission peaked at 660 was attributed to phosphorescence from the Pt(II) porphyrin cores, while the minor high-energy emission bands at 540 and 590 nm were suggested to be derived from thermally populated triplet states ("hot bands") or singlet states generated by TTA.

The data from devices prepared by spin coating these dendrimers as the non-doped emissive layer are better than those of small molecule Pt(II) porphyrin analogs.

The emission of platinum(II) porphyrin complexes can be further shifted to the NIR region by extending the π conjugation of the porphyrin ligand [30]. Schanze and co-workers developed a series of NIR-emitting platinum(II) di- and tetra-substituted benzoporphyrin complexes, **Pt-6–8** (**Figure 2**), to investigate structure-property relationships and the link between photophysical parameters and OLED performances. The photophysical parameters are listed in **Table 1**. Although the di-substituted porphyrin complex gives a higher Φ_{PL} (0.49) and longer τ_{em} (53.0 μs) than the tetra-substituted complexes (Φ_{PL} = 0.33–0.35; τ_{em} = 29.9–32.0 μs) in solution, the same trend does not hold in solid matrices, in which the emission lifetimes of **Pt-6–8** are comparable (45.7–57.5 μs). The EQEs of all the devices (8.0–9.2%) were similar. Consequently, the authors concluded that (i) the major non-radiative decays are associated with out-of-plane distortion of the porphyrin ligands, (ii) the rigid polymer matrix could help suppress the enhanced non-radiative decay of the more distorted complexes (**Pt-6** and **Pt-7**) in solid matrices, and (iii) the performance of platinum(II) benzoporphyrin-based OLEDs was observed to strongly correlate with the emission lifetime in the solid matrix.

Pt(II) porphyrins as OLED emitters generally exhibit high thermal stability and outstanding performance in saturated red and NIR devices in terms of color purity and EL efficiencies attributed to their narrow emission band and high emission quantum yields. Nevertheless, the practical interest of this class of Pt(II) emitters is limited by the long emission decay times, which would result in substantial efficiency loss at higher luminance. It is hypothesized that careful device design and the use of appropriate auxiliary materials to mitigate TTA, e.g., by using a double host to broaden the recombination zone, could be a strategy for improving the practicality of these materials.

3.2 Platinum(II) complexes supported by dianionic N_2O_2 ligands

3.2.1 Ligand systems and photophysical properties

Using "one-metal-one-ligand" approach to construct a stable luminescent platinum material, Che and co-workers developed the first non-porphyrin tetradentate aromatic N_2O_2 chelates, **Pt-9** and **Pt-10** (**Figure 3**), in 2003 [31]. The photophysical data of **Pt-9**-**12** are summarized in **Table 2**. These aromatic diimine-based Pt(II) complexes exhibit intense absorption bands at λ < 375 nm, which are attributed to

Complex	Φ_{PL} toluene	τ_{em} (μs) toluene	τ_{em} (μs) film	λ_{max} EL (nm)	Max EQE (%)
Pt-1	0.42	80.5	91.0[a]	650	4.0
Pt-2	0.09[b]	60.0[b]	—	655	—[c]
Pt-6	0.35	29.9	45.7[d]	773	8.0 ± 0.5
Pt-7	0.33	32.0	49.8[d]	773	9.2 ± 0.6
Pt-8	0.49	53.0	57.5[d]	777	7.8 ± 0.5

[a] *In polystyrene.*
[b] *In CH_2Cl_2.*
[c] *Max PE = 0.90 lm W^{-1}.*
[d] *In PVK:PBD.*

Table 1.
*Photophysical and OLED performance data for **Pt-1**, **Pt-2**, and **Pt-6–8**.*

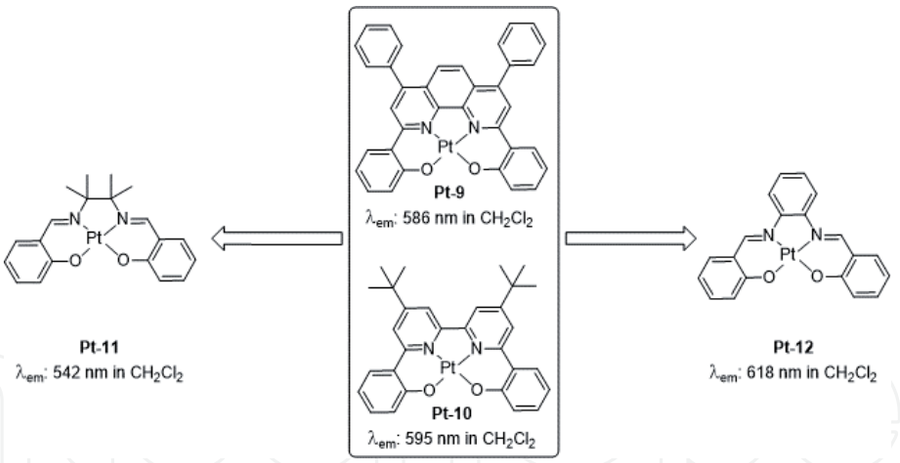

Figure 3.
Chemical structures of the platinum(II) complexes supported by dianionic N_2O_2 ligands, ***Pt-9–12****.*

		Emission		
Complex	**UV-Vis absorption in CH_2Cl_2, λ_{abs} (nm) (298 K) (ε, $\times 10^4$ $mol^{-1}dm^3cm^{-1}$)**	**λ_{em} (nm)**	**τ_{em} (μs)**	**Φ_{PL}**
Pt-9	291 (3.92), 315 (3.40), 325 (3.23), 352 (2.58), 375 (2.47), 420 (0.52), 488 (sh, 0.67), 504 (0.72)	586	5.3	0.60
Pt-10	253 (4.10), 313 (1.84), 397 (0.840), 479 (0.294), 504 (sh, 0.252)	595	1.9	0.12
Pt-11	319 (1.31), 344 (1.67), 420 (0.58), 440 (0.54)	542	3.7	0.27
Pt-12	253 (4.16), 318 (2.49), 366 (3.61), 382 (3.41), 462 (0.93), 503 (sh, 0.86), 535 (0.99)	618	3.6	0.20

Table 2.
Photophysical data of ***Pt-9–12****.*

ligand-centered $^1\pi$-π^* transitions. The low-energy absorptions between 400 and 500 nm are assigned to the ^{1}ILCT transition (L → π^*, L = lone pair/phenoxide) mixed with ^{1}MLCT [dπ → π^*(diimine)] character. **Pt-9** and **Pt-10** display strong orange-red phosphorescence in CH_2Cl_2 at 298 K with λ_{max} values of 586 and 595 nm, respectively. The emission lifetimes and quantum yields are 5.3 μs and 0.6 for **Pt-9** and 1.9 μs and 0.1 for **Pt-10**. Owing to the ^{3}MLCT/^{3}ILCT nature of the emissive state, the emission lifetimes of **Pt-9** and **Pt-10** are significantly shorter than those of the aforementioned platinum(II) porphyrin complexes.

Schiff base ligands constitute another important class of N_2O_2 systems. The facile synthesis of Schiff base ligands, which can be prepared via one-pot multi-gram scale condensation reactions between substituted salicylic aldehydes and alkyl/aryl diamines, makes them an attractive ligand system for use in the synthesis of Pt(II) emitters. To elucidate structure-property relationships, Che and co-workers conducted a detailed investigation of a panel of Pt(II) Schiff base complexes with alkylene and arylene bridges (e.g., **Pt-11** and **Pt-12**; **Figure 3**) [32, 33]. The photophysical parameters are listed in **Table 2**. Similar to **Pt-9** and **Pt-10**, the absorption bands at λ < 400 nm are dominated by ligand-based $^1\pi$-π^* transitions, while those at λ > 400 nm are attributed to ^{1}MLCT and ^{1}ILCT [L → π^*] transitions. **Pt-11**, bearing a (tetramethyl)ethylene bridge, shows yellow-green emissions (λ_{em} = 541–546 nm) in solution with τ_{em} values of 3.4–3.9 μs and Φ_{PL} values of 0.18–0.27. When the nonconjugated bridge was replaced with a conjugated phenylene unit, as in **Pt-12**, a significant redshift in the emission λ_{max} to 608–628 nm in

various solvents with τ_{em} values of 1.4–3.6 μs and Φ_{PL} of 0.10–0.26 was observed. In addition, the emission color can be finely tuned by attaching electron-donating or electron-withdrawing substituent(s) to the phenolate moieties of Schiff base ligands. The emission of these complexes displays moderate solvatochromic shift, and the emissive states were assigned to have mixed ^{3}ILCT [L → π*(diimine)] and ^{3}MLCT [d → π*(diimine)] characters. This assignment was further corroborated by the intermediate magnitude of their total zero-field spitting (ZFS) values between 14 and 28 cm^{-1}. These ZFS values lie between those of conventional Ru(II), Os(II), and Ir(III) ^{3}MLCT emitters (60–170 cm^{-1}) and those of Pd(II) and Rh(III) ^{3}IL emitters with ZFS < 1 cm^{-1}.

3.2.2 Chemical and thermal stability

Platinum(II) N_2O_2 complexes are generally stable in the solid state under ambient conditions. When dissolved in solution and exposed to light and air, **Pt-9** and **Pt-10** gradually decompose. By contrast, all Schiff base complexes are stable in common organic solvents such as EtOH, 2-propanol, DMSO, and CH_3CN under ambient conditions. All platinum(II) N_2O_2 complexes exhibit high thermal stability as assessed by thermal gravimetric analysis; **Pt-9** and **Pt-10** are stable up to 440 and 530°C, respectively. The decomposition temperatures of Pt(II) Schiff base complexes, including **Pt-11** and **Pt-12**, are in the range of 315–495°C. The introduction of **–**CH_3, *t*-Bu, or -F to the phenoxide moieties positively influenced the thermal stability of Pt(II) Schiff base complexes.

3.2.3 Electroluminescent properties

Devices with bis(2-(2-hydroxyphenyl)pyridine)beryllium ($Bepp_2$) as the host and **Pt-9** or **Pt-10** dopant as the emitting layer were fabricated: [ITO/N,N′-di(α-naphthyl)-N,N-diphenyl-(1,1-biphenyl)-4,4-diamine (NPB, 30 nm)/$Bepp_2$:**Pt-9** (or **Pt-10**) (30 nm)/LiF (0.5 nm)/Al (250 nm)]. All of the devices exhibited turn-on voltages ranging from 5 to 7 V, with yellow to yellow-green emissions. **Pt-10** showed a maximum luminance and power efficiency of 9330 cd m^{-2} (at 330 mA cm^{-2}) and 1.44 lm W^{-1} (at 40 mA cm^{-2}), respectively. Notably, although **Pt-9** exhibited a much higher emission quantum yield than **Pt-10** in solution, the EL performance of the former was inferior to that of the latter, which was attributed to the strong intermolecular quenching processes in **Pt-9**. Therefore, the bulky *t*-Bu groups in **Pt-10** are thought to play a vital role in suppressing intermolecular interactions.

The EL properties of platinum(II) Schiff base complexes were investigated. **Figure 4** shows two additional complexes, **Pt-13** and **Pt-14** [33, 34], discussed below, together with **Pt-11** and **Pt-12**. The EL spectra of devices with 4,4′-bis(carbazol-9-yl)biphenyl (CBP) as the host closely matched the corresponding PL spectra, suggesting that the EL originated from the same triplet excited states. The best device performances were obtained with dopant concentrations ranging from 1.5 to 4.5 wt%. At low dopant concentrations (<5.0 wt%), the devices exhibited yellow-green emission, and the efficiency was improved with increasing dopant concentrations. Additionally, the profile of the emission spectra remained unchanged. With doping concentration >5 wt%, the current efficiency (CE) was found to decrease, and the emission color changed due to the formation of excimers or aggregates. A maximum luminance of 9370 cd m^{-2} was achieved by optimizing the dopant concentration to 3 wt%. Notably, devices with simple structures, with $Bepp_2$ as the host and **Pt-13** as the dopant, can generate white emission, and the maximum luminance reached 3045 cd m^{-2}. Additionally,

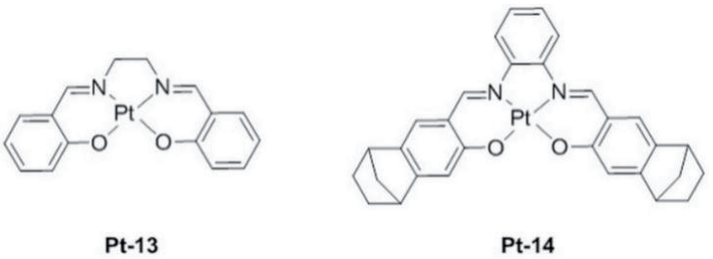

Figure 4.
*Chemical structures of platinum(II) Schiff base complexes **Pt-13** and **Pt-14**.*

the CIE coordinates of (0.33, 0.35) are close to those of white light (0.33, 0.33). Unlike **Pt-13**, no aggregate or excimer formation was observed for devices with 6.0 wt% of **Pt-11**, presumably due to the steric bulk of the (tetramethyl)ethylene bridges. Consequently, the performance of **Pt-11** was superior to that of **Pt-13**, with current and power efficiencies and luminance values up to 31 cd A^{-1}, 14 lm W^{-1}, and 23,000 cd m^{-2}, respectively, which are comparable to those of tris-cyclometalated iridium(III) complexes.

For red light-emitting materials, **Pt-12** achieved a current efficiency of 10.8 cd A^{-1} and an operational lifetime of >20,000 h at 100 cd m^{-2}. To suppress the intermolecular interactions as well as further optimize EL performance, a norbornene-based platinum(II) Schiff base complex, **Pt-14** (**Figure 4**) [34], was prepared. Sterically hindered norbornene moieties are highly effective in mitigating emission self-quenching. At a luminance of 1000 cd m^{-2}, **Pt-14** showed a current efficiency approximately 50% higher than that of **Pt-12** with the same device structure. In addition, the efficiency roll-off was reduced by 35%, benefiting from the lower self-quenching rate constant. By incorporating a wide bandgap iridium(III) complex as a co-dopant, high current and power efficiencies of 20.43 cd A^{-1} and 18.33 lm W^{-1}, respectively, were realized. In addition, the current efficiency could be maintained at 14.69 cd A^{-1} at a high luminance (1000 cd m^{-2}). More importantly, an operational lifetime of 18,000 h was realized at an initial luminance of 1000 cd m^{-2}, demonstrating that platinum(II) Schiff base complexes are promising red emitters for OLED displays.

Ease of synthesis, relatively short emission lifetime, high thermal stability, and decent emission quantum yield are traits that make platinum(II) N_2O_2 emitters attractive phosphorescent dopants, particularly for red OLEDs. Further research efforts in assessing and optimizing their operational stability in devices are anticipated.

3.3 Platinum(II) complexes supported by cyclometalated ligands

Incorporating anionic C-donor unit(s) into chromophoric ligands has been recognized as an effective strategy to enhance the luminescence of d^6 and d^8 transition metal complexes [35]. The same principle generally holds for tetradentate Pt(II) emitters. The tetradentate cyclometalated Pt(II) emitters reported in the literature typically feature high phosphorescence quantum yields of up to unity, which could be attributed to the following combined effects: (i) the rigid tetradentate ligand scaffold may help suppress excited-state structural distortion, thereby disfavoring non-radiative deactivation of the emissive excited state, (ii) the strongly σ-donating carbanion may destabilize the antibonding Pt $5d_{x2-y2}$ orbitals to a great extent, thus reducing the quenching of emissive states via the ^{3}d-d state, and (iii) the carbanion donor atom may also increase the metal character (e.g., ^{3}MLCT) and hence the radiative decay rate of the emissive excited states.

3.3.1 Pt(II) emitters with [O^N^C^N] ligands

In 2013, Che et al. developed the first phosphorescent platinum(II) complexes supported by tetradentate [O^N^C^N] ligands for white OLED and polymer organic light-emitting diode (PLED) applications [36]. These complexes were found to possess desirable physical properties as OLED emitters including high thermal stability with T_d > 400°C and ease of sublimation for vacuum deposition. Several follow-up studies on this family of Pt(II) emitters for high-efficiency OLEDs have been reported by the same group [22, 37–39].

3.3.1.1 Molecular design strategies

In general, for monochromic blue to yellow OLEDs, emission from monomeric Pt(II) complexes should be dominant, and aggregate emission should be minimized for achieving a high color purity (**Figure 5**). Early works showed that platinum(II) [O^N^C^N] complexes are prone to excimeric emission at elevated concentration. In attempts to address the excimer issues for realizing monchromic green and yellow OLEDs, Che and co-workers proposed a strategy to bolster the 3D configuration of the moelcular strucutre of the complexes to supress the intermolecular interactions via the introduction of rigid and bulky substituents, such as t-Bu groups and a norbornene moiety, to the ligand periphery, and the incorporation of bridging tertiary arylamine units or biphenyl groups with spiro linkages to the ligand frameworks. These modifications were found to effectively disfavor intermolecular interactions, evident by the diminished emission self-quenching and excimeric emissions in solution and in thin film at high concentrations. In addition, the corresponding devices showed improved device efficiencies and diminished efficiency roll-offs. Additionally, Pt(II) [O^N^C^N] emitters bearing a cross-shaped molecular structure (i.e., a spiro linkage) may also cause molecular entanglement in the amorphous state, which help prevent recrystallization of the emissive layer and prolong operational lifetimes.

Through deliberate molecular design and variations in the doping concentration, the extent of intermolecular interactions and aggregations of platinum(II) [O^N^C^N] emitters could be controlled and manipulated for red and NIR as well as white OLED applications based on aggregation and monomer/aggregation emissions, respectively (**Figure 5**). Instead of tuning the 3D configuration to limit intermolecular interactions, for these applications, adopting a relatively planar ligand scaffold and introducing fluorine substituent(s) at specific position(s),

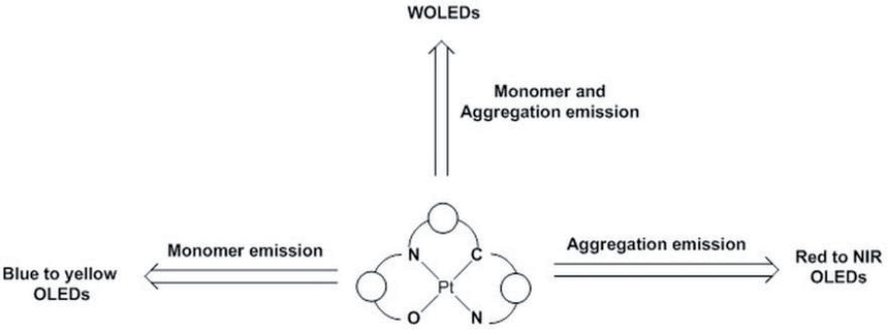

Figure 5.
Molecular design strategies for various OLED applications.

which favor intermolecular π-π and/or Pt-Pt interactions for low-energy aggregate emission from the excited states of dimers or oligomers, are preferred.

3.3.1.2 Photophysical properties and OLEDs based on monomer emission

The cyclometalated [O^N^C^N] ligand system is useful for the construction of robust and highly efficient Pt(II) emitters. Che et al. developed a panel of platinum(II) [O^N^C^N] emitters, i.e., **Pt-15**–**Pt-20** (**Figure 6**) [39], and systematically investigated their photophysical and electroluminescent properties, which are summarized in **Tables 3** and **4**.

The intense absorption bands of **Pt-15**–**20** at <300 nm are assigned to intraligand π-π* transitions, and the moderately intense bands at 430–450 nm with weak absorption at >460 nm are assigned to transitions with mixed MLCT and ILCT character. In degassed CH_2Cl_2 solutions, complexes **Pt-15**–**18** exhibit strong green to yellow luminescence (λ_{em} = 522–570 nm) with emission quantum yields and lifetimes in the range of 0.23–0.95 and 2.3–5.5 μs, respectively. With an additional t-Bu group at the *ortho*-position of the phenolate unit, **Pt-18** shows a much lower emission quantum yield (0.23) than **Pt-15**–**Pt-17** (0.77–0.95), indicating that the free rotation of this t-Bu group contributes to the increased non-radiative decay of the emissive state. Congeners **Pt-19** and **Pt-20**, with 6-5-6 metallacycles, are also highly efficient yellow (λ_{em} = 551 nm) and green (λ_{em} = 517 nm) phosphors, respectively. Their solution emission quantum yields (>0.80) and lifetimes (<5.1 μs) are similar to those of **Pt-15**–**17**. Femtosecond time-resolved fluorescence (fs-TRF) measurements suggested that **Pt-19** and **Pt-20** undergo an ultrafast intersystem crossing process with time constants of 0.44 and 0.15 ps, respectively. The emission origin for **Pt-15**–**20** was assigned to excited states with mixed ^{3}MLCT and $^3[L \rightarrow \pi^*]$ characters. Notably, **Pt-17**–**Pt-20** do not display excimer emissions in CH_2Cl_2 even at high concentrations (1.0×10^{-4} M), while **Pt-15** and **Pt-16** showed excimer emissions as a low-energy band (ca. 650 nm) under the same conditions. This finding suggests that the incorporation of a bridging tertiary amine or a spiro-fluorene linkage in the ligand framework would be as effective in suppressing the intermolecular

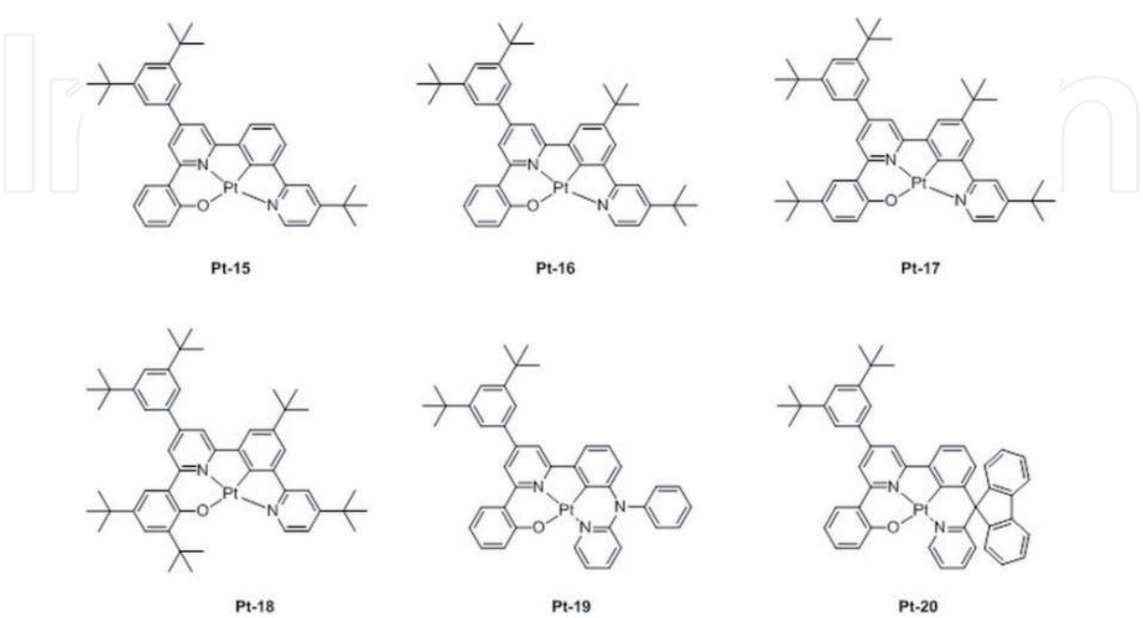

Figure 6.
Chemical structures of platinum(II) complexes ***Pt-15–20****.*

		Emission		
Complex	**UV-Vis absorption in CH_2Cl_2, λ_{abs} (nm) (ε, $\times 10^4$ $mol^{-1}dm^3cm^{-1}$)**	**λ_{em} (nm)**	**τ_{em} (μs)**	**Φ_{PL}**
Pt-15	282 (4.5), 304 (sh, 3.3), 336 (sh, 1.8), 372 (1.9), 400 (sh, 1.1), 430 (sh, 0.8)	522	4.0	0.77
Pt-16	283 (4.4), 298 (sh, 3.7), 362 (sh, 1.6), 373 (1.7), 400 (sh, 1.0), 435 (sh, 0.69)	522	4.0	0.77
Pt-17	286 (4.4), 303 (sh, 3.2), 265 (sh, 1.5), 376 (1.8), 405 (sh, 0.98), 440 (sh, 0.75)	543	5.5	0.95
Pt-18	261 (5.1), 288 (5.4), 361 (sh, 1.5), 376 (2.2), 410 (sh, 1.2), 450 (sh, 0.85)	570	2.3	0.23
Pt-19	262 (4.4), 295 (sh, 3.5), 330 (2.2), 370 (sh, 1.1), 450 (sh, 0.27), 481 (sh, 0.21)	551	4.3	0.90
Pt-20	261 (sh, 5.0), 279 (5.4), 301 (sh, 3.6), 329 (1.8), 356 (1.7), 393 (0.72), 431 (sh, 0.38)	517	5.1	0.80

Table 3.
*Photophysical data of **Pt-15**–**Pt-20**.*

interactions/aggregation as introducing multiple bulky t-Bu substituents at the ligand periphery.

The EL properties of **Pt-15**–**Pt-18** were investigated in OLEDs based on the device structure [ITO/MoO_3 (5 nm)/di-[4-(N,N-ditolylamino)-phenyl]cyclohexane (TAPC, 50 nm)/4,4′,4″-tris(carbazole-9-yl)triphenylamine (TCTA):platinum complex (10 nm)/1,3,5-tri(m-pyrid-3-yl-phenyl) (TmPyPB, 50 nm)/LiF (1.2 nm)/Al (150 nm)], in which the emission layer was doped with **Pt-15**–**18** at different concentrations. The EL performance data are summarized in **Table 4**. At low doping concentrations, the EL spectra of all devices matched well with the corresponding solution-phase monomer emissions. With increasing dopant concentrations, aggregation emission was observed for **Pt-15**–**Pt-17**. Notably, aggregation emission was not observed for **Pt-18**, even at a high doping concentration of 15 wt%, revealing that the self-aggregation of **Pt-18** in EML is negligible. At an optimized doping concentration of 10 wt%, **Pt-18** achieved a maximum EQE of 27.1%, and this value dropped to 16.8% at a luminance of 10,000 cd m^{-2}.

The EL properties of **Pt-19** and **Pt-20** were studied in a device with the structure [ITO/MoO_3 (5 nm)/TAPC (50 nm)/TCTA:platinum(II) complex (10 nm)/TmPyPB or 2,4,6-tris(3-(3-(pyridin-3-yl)phenyl)phenyl)-1,3,5-triazine (Tm3PyBPZ, 50 nm)/LiF (1.2 nm)/Al (150 nm)] in which the doping concentration of the complexes ranged from 2 to 30 wt%. Similar to **Pt-15**–**Pt-18**, at a low doping concentration of 2 wt%, the emissions of both complexes are identical to the corresponding monomer emissions in solution. Increasing the doping concentration to 30 wt% caused a slight redshift for the **Pt-19**-based device, whereas only monomer emission was observed for **Pt-20** at the same doping level. This phenomenon could be rationalized by **Pt-19** to be more prone to undergo intermolecular interactions than those of **Pt-20**. In TmPyPB devices, a maximum EQE of 27.6%, CE of 104.2 cd A^{-1}, and PE of 109.4 lm W^{-1} have been achieved with 10 wt% **Pt-20**, and a maximum EQE of 26.0%, CE of 100.0 cd A^{-1}, and PE of 105.5 lm W^{-1} were achieved with **Pt-19** under the same conditions. At a high luminance (10,000 cd m^{-2}), the EQE of the devices based on **Pt-19** (30 wt%) or **Pt-20** (10 wt%) remained above 20%. To further optimize the PE of the OLEDs, TmPyPB was replaced with Tm3PyBPZ as the ETL. In Tm3PyBPZ devices, the driving voltage was significantly decreased. Consequently, the maximum PEs were improved to 118

	PE (lm W^{-1})		CE (cd A^{-1})		EQE (%)		
Complex (wt%)[a]	**Max.**	**At 10^4 cd m^{-2}**	**Max.**	**At 10^4 cd m^{-2}**	**Max.**	**At 10^4 cd m^{-2}**	**CIE (x, y)**
Pt-15 (2)	92.0	21.8	83.4	55.0	24.4	16.4	(0.32, 0.63)
Pt-15 (6)	25.2	5.2	25.5	16.4	13.5	8.6	(0.48, 0.50)
Pt-15 (12)	6.7	1.3	11.1	5.3	10.9	5.2	(0.60, 0.40)
Pt-16 (4)	61.5	10.5	68.3	31.4	19.7	8.6	(0.34, 0.62)
Pt-16 (8)	60.0	16.8	75.0	46.6	20.6	13.1	(0.35, 0.62)
Pt-16 (16)	48.6	16.1	51.0	43.4	20.4	17.1	(0.42, 0.56)
Pt-17 (2)	98.1	20.0	93.7	46.0	23.8	11.2	(0.39, 0.60)
Pt-17 (10)	94.3	32.1	90.0	68.1	24.8	18.8	(0.39, 0.60)
Pt-17 (15)	65.3	23.2	72.7	51.2	21.8	15.4	(0.40, 0.58)
Pt-18 (4)	82.1	7.4	86.1	22.8	22.7	6.6	(0.41, 0.57)
Pt-18 (10)	86.4	26.5	100.5	62.8	27.1	16.8	(0.41, 0.57)
Pt-18 (16)	91.0	32.6	94.0	73.8	26.3	19.1	(0.43, 0.56)
Pt-19 (2)	103.3	12.8	96.3	40.2	25.7	11.4	(0.42, 0.57)
Pt-19 (10)	105.5	20.6	100.0	55.4	26.0	14.4	(0.44, 0.55)
Pt-19 (16)	101.3	27.7	96.8	70.4	25.7	18.7	(0.45, 0.54)
Pt-19 (30)	80.7	27.8	82.5	68.4	24.8	20.5	(0.47, 0.52)
Pt-20 (2)	99.6	12.6	91.7	34.7	24.9	9.59	(0.29, 0.64)
Pt-20 (6)	106.7	31.1	101.1	73.1	26.9	19.1	(0.31, 0.64)
Pt-20 (10)	109.4	24.7	104.2	79.2	27.6	20.0	(0.31, 0.64)
Pt-20 (30)	95.7	28.4	90.0	66.9	24.0	17.9	(0.33, 0.63)
Pt-19 (10)[b]	118.0	22.5	94.3	48.0	25.3	12.5	(0.44, 0.55)
Pt-20 (10)[b]	126.0	24.4	98.8	52.0	26.4	13.6	(0.31, 0.63)

[a] *TmPyPB is used as the ETL.*
[b] *Tm3PyBPZ is used as the ETL.*

Table 4.
OLED performance data for ***Pt-15–Pt-20****.*

and 126 lm W^{-1} for the devices with **Pt-19** and **Pt-20** as dopants, respectively, and these values are comparable to those of the best iridium(III) OLED devices without out-coupling enhancement.

3.3.1.3 Aggregation-induced red and NIR OLEDs

The emission of Pt(II) complexes in aggregation forms is dramatically redshifted from that of monomers. Because of the increased metal character in the excited states (e.g., MMLCT) leading to the enhanced radiative decay rates, the emission lifetimes of aggregated Pt(II) emitters are usually short, in the range of 0.1–1 μs, which is fundamentally important for addressing the efficiency roll-off and the operational lifetime issues of phosphorescent OLEDs. In addition, this aggregation emission can be manipulated by tuning the doping concentration; this is particularly useful for the design of high-performance red and NIR OLEDs.

Recently, two series of platinum [O^N^C^N] complexes (**Figures 6** and 7), i.e., type-I (**Pt-21** and **Pt-22**) and type-II (**Pt-15**, **Pt-16** and **Pt-23**) [39, 40], which are prone to excited-state aggregation, were employed as emitting material in both doped and non-doped deep red and NIR devices; these complexes exhibited high EQE and low efficiency roll-off. For devices with neat complexes, high emission quantum yields were only realized with type-I complexes. For instance, when using a neat **Pt-21** film as the EML, the device demonstrated NIR emission with λ_{max} exceeding 700 nm and with an EQE of 15.84%. In addition, the EQE remained at 11.19% even at a high current density of 100 mA cm^{-2}. Of the doped devices, the device based on **Pt-16** (26 wt%) exhibited a deep red emission with λ_{max} of 661 nm, CIE coordinates of (0.63, 0.37), and an EQE value of 21.75% at a luminance of 1000 cd m^{-2}. The operational lifetimes at 90% initial luminance (LT90, L_0 = 100 cd m^{-2}) with 10 and 30 wt% **Pt-23** as the dopant were 59 and 374 h, respectively, demonstrating that aggregation-based devices would have longer lifetimes.

3.3.1.4 WOLEDs based on a single emitter

WOLED devices typically employ two or more co-dopants with different emission colors in the EML. Nevertheless, broad-band white light emission with a single Pt(II) emitter could be achieved when both the high-energy monomer emission and low-energy aggregation emission are harvested. In this case, a fine balance of the concentration of excited state monomers and excited state aggregation species is desired. Complex **Pt-22** displays both high-energy monomer emission at 482 nm and low-energy emission at 633–650 nm with emission quantum yields of up to 0.78 when doped into a solid matrix beyond 1.5 wt% [41]. This complex was first reported and used as a single emitter in white PLEDs by Che et al., and white

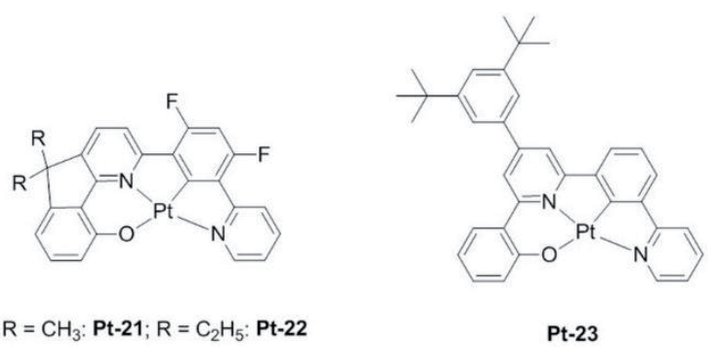

R = CH_3: **Pt-21**; R = C_2H_5: **Pt-22**

Pt-23

Figure 7.
*Chemical structures of platinum(II) complexes **Pt-21–Pt-23**.*

emission with an EQE of 11.51%, CIE coordinates of (0.41, 0.45), and a CRI of 74 at 1000 cd m^{-2} were realized with 16 wt% **Pt-22** as the dopant. To further optimize the performance of WOLEDs, devices with a structure of [ITO/MoO_3 (5 nm)/TAPC (50 nm)/host:7 wt% 7 (10 nm)/EML (50 nm)/LiF (1.2 nm)/Al (150 nm)] were fabricated. In these devices, 9-[3-[6-(3-carbazol-9-ylphenyl)pyridin-2-yl]phenyl] carbazole (26DCzppy) or TCTA/26DCzppy (1:1 in weight) was used as a single or double host, while TmPyPB or Tm3PyBPZ was used as the ETL. The EQE of the TmPyPB device dropped slightly with increasing luminance. To decrease the driving voltage, 26DCzppy was replaced with TCTA/26DCzppy (1:1 w/w), and the turn-on voltage was decreased from 3.5 to 3.0 V, resulting in an EQE of 23.2%. The turn-on voltage was further decreased to 2.7 V by replacing TmPyPB with Tm3PyBPZ. Consequently, the PE of the device reached a high value of 55.5 lm W^{-1}, which is comparable to the best reported values for a single emitter.

3.3.2 Pt(II) emitters with [N^C^C^N] ligands

In 2013, Li et al. developed two efficient blue-emitting tetradentate platinum complexes with a carbazolyl-pyridine motif integrated into the ligand scaffold. These complexes show emission quantum yields of up to 0.89, and the corresponding devices achieved excellent EQEs of up to 25%, highlighting the potential of these platinum emitters for blue OLED applications [42]. Subsequent works by the same group demonstrated that the carbazolyl-pyridine entity is also a versatile modular building block for various tetradentate dianionic cyclometalated N^C^C^N ligands, providing access to several new classes of efficient blue-, green-, and red-emitting platinum(II) complexes [43–46].

3.3.2.1 Molecular design strategies

The emission energies of the complexes in this family can be rationally and readily tuned by modifying the modular ligand scaffold, which consists of a cyclometalated chromophoric C^N unit and an auxiliary carbazolyl-pyridine group connected by a heteroatom or the heteroatom itself may be part of the chromophoric unit, as shown in **Figure 8**. Complex **Pt-24**, bearing a 4-phenylpyridine ring, shows red emission at 602 nm in solution at rt. Upon switching the 4-phenylpyridine group in the chromophoric unit to a pyrazole moiety to raise the LUMO energy, the emission of **Pt-25** is considerably blueshifted to 491 nm. The emission energy of the complexes can be further increased by reducing or breaking the π conjugation via manipulation of the chromophoric unit and/or the tethered group (**Pt-26**–**28**). For instance, by replacing carbazole with a 9,10-dihydroacridine group to interrupt the π conjugation, the emission maximum of **Pt-28** is blueshifted by 8 nm to 483 nm with respect to **Pt-25**.

This class of Pt[N^C^C^N] complexes was reported to be free from excimer-based emission, which was proposed to be a consequence of distortion of the molecular structure from planarity that disfavors intermolecular interactions [47]. Recently, Li and co-workers conducted a systematic photophysical study on derivatives of **Pt-25** and found that introducing substituents on the auxiliary unit dramatically influenced the emission spectral bandwidth and the nature of the emissive T_1 state through modulating the degree of mixing of ^{1}MLCT/^{3}MLCT characters with ^{3}IL state [48].

3.3.2.2 Red-emitting complexes and devices

Pt-24 is a representative red-emitting complex in this family [44]. This complex shows strong absorption bands at 250–400 nm (ε = 2.4–6.4 × 10^4 cm^{-1} M^{-1}) attributable to $^1\pi$–π^* transitions localized on the cyclometalated tetradentate ligand.

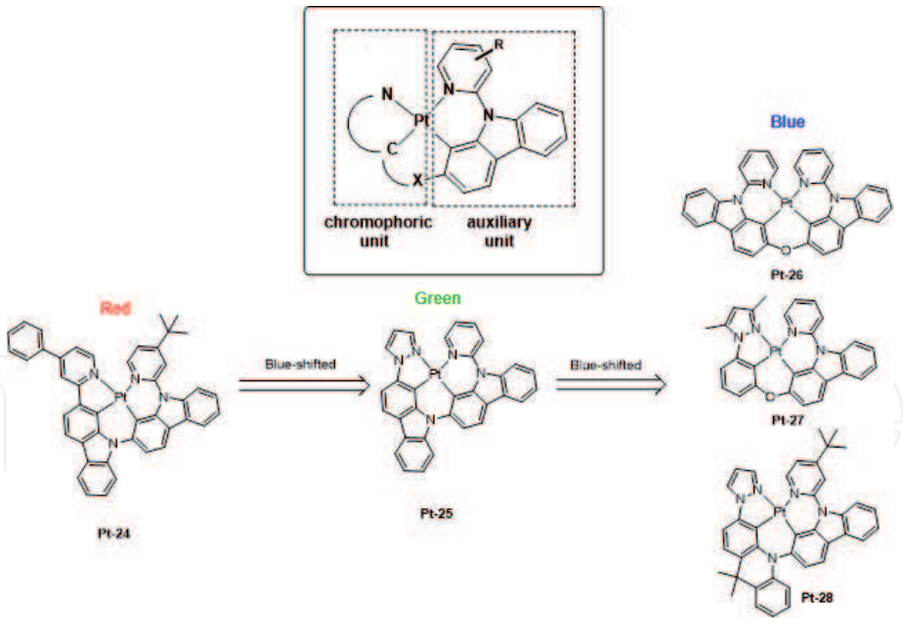

Figure 8.
Molecular design strategies for color tuning.

The moderately intense absorption, which can be assigned to the ^{1}MLCT transition appears at a longer wavelength of 450–550 nm (ε = 3900 cm^{-1} M^{-1}). Spin-forbidden triplet absorption is located beyond 560 nm (ε = 120 cm^{-1} M^{-1}) in CH_2Cl_2. **Pt-24** shows red emission at 602 nm in CH_2Cl_2 with an emission quantum yield of 34% at room temperature. A significant rigidochromic blueshift by ca. 30 nm to 574 nm is observed in the glassy solution (2-MeTHF) at 77 K, which is a sign of strong mixing of ^{1}MLCT/^{3}MLCT characters in the T_1 state.

The EL properties of **Pt-24** were studied with a device structure of [ITO/dipyrazino[2,3-f:2′,3′-h]quinoxaline-2,3,6,7,10,11-hexacarbonitrile (HATCN, 10 nm)/NPB (40 nm)/10% **Pt-24**:CBP (25 nm)/BAlq (10 nm)/Alq_3 (40 nm)/LiF (1 nm)/Al (100 nm)], where BAlq is bis(2-methyl-8-quinolinolato)(biphenyl-4-olato)aluminum. The device showed an orange-red emission band at 606 nm, and this band was broader than that in solution. The EL spectrum also included a weak blue emission between 450 and 550 nm, originating from the hole transporting layer NPB. The device displayed a maximum EQE of 8.2% and an EQE of 7.8% at a luminance of 100 cd m^{-2}, which is not outstanding among the reported red-emitting metal complexes. However, the operational lifetime was encouraging. At an initial luminance of 1000 cd m^{-2}, the operational lifetime at 97% of the initial luminance (LT_{97}) was approximately 534 h, which is comparable to that of well-known iridium complexes with similar device structures, e.g., $Ir(ppy)_3$ and $(pq)_2Ir(acac)$. To remove the NPB emission as well as improve the efficiency, a 10-nm thick layer of 9,9′,9″-triphenyl-9H,9′H,9″H-3,3′:6′3″-tercarbazole (TrisPCz), with a higher LUMO level and triplet energy than the CBP host, was disposed between the HTL and EML. The maximum EQE was further increased to 11.8%, and the operational lifetime of LT_{97} was estimated to be 542 h at a luminance of 1000 cd m^{-2}. In addition, by replacing Alq_3 with 2,7-di(2,2′-bipyridin-5-yl)triphenylene (BPyTP), a device with the structure of [ITO/HATCN (10 nm)/NPB (40 nm)/TrisPCz (10 nm)/10% **Pt-24**:CBP (25 nm)/BAlq (10 nm)/BPyTP (40 nm)/LiF (1 nm)/Al (100 nm)] was fabricated to decrease the driving voltage. Notably, the device showed a driving voltage of 3.6 V at a current density of 1 mA cm^{-2}, which was 1.6 V lower than that of the above devices with Alq_3 as the ETL. Importantly, the operational lifetime was also substantially improved, with an LT_{97} value of 638 h at a luminance of 1000 cd m^{-2}.

3.3.2.3 Green-emitting complexes and devices

Pt-25 displays strong green phosphorescence at 491 nm in CH_2Cl_2 at room temperature with emission quantum yields of 0.81 in CH_2Cl_2 and 0.90 in doped poly(methyl methacrylate (PMMA) films along with an exceptionally narrow spectral bandwidth with an full-width-at-half-maximum (FWHM) of 18 nm, which is comparable to those of quantum dots (25–40 nm) [46]. The authors attributed this phenomenon to localization of the T_1 state on the chromophoric unit.

To investigate the EL properties of **Pt-25**, OLEDs with the structure [ITO/PEDOT:PSS/NPB (30 nm)/TAPC (10 nm)/x% **Pt-25**:2,6-bis(N-carbazolyl)pyridine (26 mCPy, 25 nm)/2,8-bis(diphenylphosphoryl)-dibenzothiophene (PO15, 10 nm)/1,3-bis[3,5-di(pyridin-3-yl)phenyl] benzene (BmPyPB, 30 nm)/LiF (1 nm)/Al (90 nm)] were fabricated with dopant concentrations (x) ranging from 2 to 14%. The device with a doping concentration of 14% demonstrated a maximum EQE of 25.6%. Additionally, **Pt-25** was employed as the emitter in a device with a structure of [ITO/HATCN (10 nm)/NPB (40 nm)/x% **Pt-25**:CBP (25 nm)/BAlq (10 nm)/Alq_3 (40 nm)/LiF/Al] (x = 6, 10, and 20) to probe the operational stability. The device with a dopant concentration of 10% exhibited an operational lifetime of 70 h at 70% of the initial luminance (LT_{70}, L_0 = 2200 cd m^{-2}), corresponding to an LT_{70} of 32,000 h at an initial luminance of 100 cd m^{-2}. Additionally, in an optimized device structure of [ITO/HATCN (10 nm)/NPB (40 nm)/9-phenyl-3,6-bis(9-phenyl-9H-carbazol-3-yl)-9H-carbazole (TrisPCz; 10 nm)/10% **Pt-25**:3,3-di(9H-carbazol-9-yl)biphenyl (mCBP; 25 nm)/9,9′-(2,8-dibenzothiophenediyl)bis-9H-carbazole (mCBT; 8 nm)/BPyTP (40 nm)/LiF/Al], a maximum EQE of 22.1% and LT_{70} value of ca. 60,000 h were achieved at a luminance of 100 cd m^{-2}.

3.3.2.4 Blue-emitting complexes and devices

Breaking the π conjugation of ligand scaffolds can increase the T_1 energy for harvesting blue emission. By having all-six-membered chelate rings to interrupt the π conjugation, the O-bridged carbazolyl-pyridyl complex **Pt-26** shows a sky blue emission at 473 nm in a PMMA film with a high emission quantum yield of 0.83 and an emission lifetime of 3.8 μs [43]. A subtle disruption of π conjugation could also blueshift the emission. **Pt-28**, featuring a 9,10-dihydro-9,9-dimethylacridine subunit, displays a structured emission at 476 nm at 77 K [45], corresponding to CIE coordinates of (0.11, 0.30), which is 8 nm blueshifted from that of its carbazole analog, **Pt-25**. The **Pt-28**-doped PMMA film showed a high emission quantum yield of 0.68. Interestingly, the emission spectrum of **Pt-28** in CH_2Cl_2 at room temperature is dramatically broader than that of **Pt-25,** possibly due to the higher flexibility of the ligand.

Devices with the structure [ITO/HATCN (10 nm)/NPB (40 nm)/EBL/10% **Pt-28**:mCBP (25 nm)/HBL/BPyTP (40 nm)/LiF (1 nm)/Al (100 nm)] were fabricated and EL properties and operational lifetimes were examined. The EBL and HBL were arranged as follows: structure 1: no EBL/EML/BAlq (10 nm); structure 2: TrisPCz (10 nm)/EML/BAlq (10 nm); structure 3: no EBL/EML/mCBT (8 nm); and structure 4: TrisPCz (10 nm)/EML/mCBT (8 nm). The device with structure 1 exhibited a maximum EQE of 8.2% at a luminance of 1000 cd m^{-2}, and the LT_{70} was estimated to be 375 h at the same luminance, which corresponds to an LT_{70} value of 18,806 h at an initial luminance of 100 cd m^{-2}. Using TrisPCz to confine the electrons inside the EML, the device with structure 2 demonstrated a slightly improved peak EQE of 10.1% at 1000 cd m^{-2}, and the LT_{70} was estimated to be 416 h. Notably, when BAlq in structure 1 was replaced with a higher bandgap material (mCBT), the device with structure 3 displayed a peak EQE of 15.9%,

and the LT_{70} was significantly prolonged to 635 h at 1000 cd m^{-2} and 31,806 h at 100 cd m^{-2}. Considering the advantages of TrisPCz (EBL) and mCBT (HTL) in the above devices (i.e., structures 2 and 3), these materials were employed in structure 4. As expected, this device achieved the best efficiency, namely, a peak EQE of 17.8%. However, the operational lifetime of LT_{70} decreased to 482 h at a luminance of 1000 cd m^{-2}.

Overall, tetradentate cyclometalated Pt(II) emitters have been demonstrated to exhibit high versatility in emission color tuning across RGB colors and white light, as well as superior photophysical and electroluminescent efficiencies and respectable operational lifetimes at practical luminance levels. While the performance metrics of this class of Pt(II) emitters are comparable to that of the best reported Ir(III) emitters in many aspects, more focused efforts should be directed at reducing the radiative lifetimes of these emitters by careful molecular design, which will be instrumental in further improving the operational stability of these complexes to meet the stringent standards required for commercialization.

4. Conclusions

Substantial room for innovation remains in OLED materials research, and the development of robust, high efficiency emitters for diverse applications remains a challenge both in academia and industry. While in the past decade, tris-(bidentate chelate) iridium(III) complexes have been seemingly edging out other classes of metal phosphors, it is remarkable that tetradentate platinum(II) emitters have demonstrated high performance and are being increasingly recognized by academia and industry as a competitive alternative. Importantly, the unique aggregation behavior and the associated photophysical properties afforded by their planar coordiantion geometry distinguish platinum(II) emitters from octahedral iridium(III) emitters. The unique photophysical properties of platinum(II) emitters render them well suited for some OLED applications using simple device structures such single-dopant WOLEDs and aggregation-based red and NIR OLEDs as covered in this review. In addition, appropriate molecular design of the ligand scaffold allows the regulation of the emissive excited states and the intermolecular interactions, which consequently offers flexibility in manipulating the emission characteristics of platinum(II) emitters to cater to various OLED applications. Indeed, sustained and concerted efforts between academia and industry have already realized successful application of tetradentate Pt(II) emitters in OLED devices in an industrial setting. It is without doubt that Pt(II) emitters, after full optimization, will meet the technical specifications including operational stability, required for commercialization. We hope the perspective described herein will spur interest among stakeholders and drive further development of tetradentate Pt(II) emitters for display and lighting applications.

Acknowledgements

This work was supported by the Major Program of Guangdong Basic and Applied Research (2019B030302009), Innovation and Technology Fund (ITS/224/17FP), Hong Kong Research Grants Council (HKU 17330416), the Basic Research Program of Shenzhen (JCYJ20170412140251576, JCYJ20170818141858021, and JCYJ20180508162429786), the National Key Basic Research Program of China (2013CB834802), Innovation and Technology Commission, Centre of Machine Learning for Energy Materials and Devices, a major initiative—Artificial Intelligence and Robotics cluster under InnoHK (AIR@InnoHK).

Conflict of interest

The authors declare no conflict of interest.

Author details

Huiyang Li[1], Tsz-Lung Lam[2,3], Liangliang Yan[1], Lei Dai[1], Byoungki Choi[4], Yong-Suk Cho[4], Yoonhyun Kwak[4] and Chi-Ming Che[2,3,5*]

1 Guangdong Aglaia Optoelectronic Materials Co., Ltd, Foshan, China

2 State Key Laboratory of Synthetic Chemistry, HKU-CAS Joint Laboratory on New Materials, Department of Chemistry, The University of Hong Kong, Hong Kong SAR, China

3 Centre of Machine Learning for Energy Materials and Devices, The University of Hong Kong, Hong Kong SAR, China

4 Samsung Electronics, Organic Material Lab, SAIT, Suwon-si, Gyeonggi-do, Korea

5 HKU Shenzhen Institute of Research and Innovation, Shenzhen, P. R. China

*Address all correspondence to: cmche@hku.hk

References

[1] Tang CW, Vanslyke SA. Organic electroluminescent diodes. Applied Physics Letters. 1987;**51**:913-915. DOI: 10.1063/1.98799

[2] Kalyani NT, Dhoble SJ. Organic light emitting diodes: Energy saving lighting technology—A review. Renewable and Sustainable Energy Reviews. 2012;**16**:2696-2723. DOI: 10.1016/j.rser.2012.02.021

[3] Tsutsui T, Takada N. Progress in emission efficiency of organic light-emitting diodes: Basic understanding and its technical application. Japanese Journal of Applied Physics. 2013;**52**:110001(1-9). DOI: 10.7567/jjap.52.110001

[4] Tiwari S, Singh M, Mishra SK, Shrivastava AK. Recent progress in organic light-emitting diodes. Journal of Nanoelectronics and Optoelectronics. 2019;**14**:1215-1224. DOI: 10.1166/jno.2019.2632

[5] Zampetti A, Minotto A, Cacialli F. Near-infrared (NIR) organic light-emitting diodes (OLEDs): Challenges and opportunities. Advanced Functional Materials. 2019;**29**:1807623(1-22). DOI: 10.1002/adfm.201807623

[6] Shuai Z, Peng Q. Excited states structure and processes: Understanding organic light-emitting diodes at the molecular level. Physics Reports-Review Section of Physics Letters. 2014;**537**:123-156. DOI: 10.1016/j.physrep.2013.12.002

[7] Thejokalyani N, Dhoble SJ. Novel approaches for energy efficient solid state lighting by RGB organic light emitting diodes—A review. Renewable & Sustainable Energy Reviews. 2014;**32**:448-467. DOI: 10.1016/j.rser.2014.01.013

[8] Wang J, Zhang F, Zhang J, Tang W, Tang A, Peng H, et al. Key issues and recent progress of high efficient organic light-emitting diodes. Journal of Photochemistry and Photobiology, C: Photochemistry Reviews. 2013;**17**:69-104. DOI: 10.1016/j.jphotochemrev.2013.08.001

[9] Chou PT, Chi Y. Phosphorescent dyes for organic light-emitting diodes. Chemistry - A European Journal. 2007;**13**:380-395. DOI: 10.1002/chem.200601272

[10] Tao Y, Yang C, Qin J. Organic host materials for phosphorescent organic light-emitting diodes. Chemical Society Reviews. 2011;**40**:2943-2970. DOI: 10.1039/c0cs00160k

[11] Shahnawaz, Swayamprabha SS, Nagar MR, RAK Y, Gull S, Dubey DK, et al. Hole-transporting materials for organic light-emitting diodes: An overview. Journal of Materials Chemistry C. 2019;**7**:7144-7158. DOI: 10.1039/c9tc01712g

[12] Kulkarni AP, Tonzola CJ, Babel A, Jenekhe SA. Electron transport materials for organic light-emitting diodes. Chemistry of Materials. 2004;**16**:4556-4573. DOI: 10.1021/cm049473l

[13] Huang Q, Cui J, Veinot JGC, Yan H, Marks TJ. Realization of high-efficiency/high-luminance small-molecule organic light-emitting diodes: Synergistic effects of siloxane anode functionalization/hole-injection layers, and hole/exciton-blocking/electron-transport layers. Applied Physics Letters. 2003;**82**:331-333. DOI: 10.1063/1.1536268

[14] Li Y. Organic Optoelectronic Materials. 1st ed. Cham/Heidelberg: Springer; 2015. p. 263. DOI: 10.1007/978-3-319-16862-3

[15] Leung MK, Chang CC, Wu MH, Chuang KH, Lee JH, Shieh SJ, et al. 6-N,N-diphenylaminobenzofuran-derived pyran containing fluorescent dyes: A new class of high-brightness red-light-emitting dopants for OLED. Organic Letters. 2006;**8**:2623-2626. DOI: 10.1021/ol060803c

[16] Swanson SA, Wallraff GM, Chen JP, Zhang W, Bozano LD, Carter KR, et al. Stable and efficient fluorescent red and green dyes for external and internal conversion of blue OLED emission. Chemistry of Materials. 2003;**15**:2305-2312. DOI: 10.1021/cm021056q

[17] Ma Y, Zhang H, Shen J, Che C. Electroluminescence from triplet metal-ligand charge-transfer excited state of transition metal complexes. Synthetic Metals. 1998;**94**:245-248. DOI: 10.1016/s0379-6779(97)04166-0

[18] Baldo MA, O'Brien DF, You Y, Shoustikov A, Sibley S, Thompson ME, et al. Highly efficient phosphorescent emission from organic electroluminescent devices. Nature. 1998;**395**:151-154. DOI: 10.1038/25954

[19] Chou PT, Chi Y. Osmium- and ruthenium-based phosphorescent materials: Design, photophysics, and utilization in OLED fabrication. European Journal of Inorganic Chemistry. 2006;**2006**:3319-3332. DOI: 10.1002/ejic.200600364

[20] Zysman-Colman E, editor. Iridium(III) in Optoelectronic and Photonics Applications. Chichester, West Sussex: John Wiley & Sons, Inc; 2017

[21] Kalinowski J, Fattori V, Cocchi M, Williams JAG. Light-emitting devices based on organometallic platinum complexes as emitters. Coordination Chemistry Reviews. 2011;**255**:2401-2425. DOI: 10.1016/j.ccr.2011.01.049

[22] Li K, So GMT, Wan Q, Cheng G, Tong WY, Ang WH, et al. Highly phosphorescent platinum(II) emitters: Photophysics, materials and biological applications. Chemical Science. 2016;**7**:1653-1673. DOI: 10.1039/c5sc03766b

[23] Eastwood D, Gouterman M. Porphyrins: XVIII. Luminescence of (Co), (Ni), Pd, Pt complexes. Journal of Molecular Spectroscopy. 1970;**35**:359-375. DOI: 10.1016/0022-2852(70)90179-7

[24] Atwater BW. Substituent effects on the excited-state properties of platinum *meso*-tetraphenylporphyrins. Journal of Fluorescence. 1992;**2**:237-246. DOI: 10.1007/BF00865282

[25] Ikai M, Ishikawa F, Aratani N, Osuka A, Kawabata S, Kajioka T, et al. Enhancement of external quantum efficiency of red phosphorescent organic light-emitting devices with facially encumbered and bulky Pt (II) porphyrin complexes. Advanced Functional Materials. 2006;**16**:515-519. DOI: 10.1002/adfm.200500492

[26] Sommer JR, Shelton AH, Parthasarathy A, Ghiviriga I, Reynolds JR, Schanze KS. Photophysical properties of near-infrared phosphorescent π-extended platinum porphyrins. Chemistry of Materials. 2011;**23**:5296-5304. DOI: 10.1021/cm202241e

[27] Retsek JL, Medforth CJ, Nurco DJ, Gentemann S, Chirvony VS, Smith KM, et al. Conformational and electronic effects of phenyl-ring fluorination on the photophysical properties of nonplanar dodecaarylporphyrins. The Journal of Physical Chemistry. B. 2001;**105**:6396-6411. DOI: 10.1021/jp004556k

[28] Che CM, Hou YJ, Chan MCW, Guo J, Liu Y, Wang Y. Meso-tetrakis(pentafluorophenyl)

porphyrinato platinum(II) as an efficient, oxidation-resistant red phosphor: Spectroscopic properties and applications in organic light-emitting diodes. Journal of Materials Chemistry. 2003;**13**:1362-1366. DOI: 10.1039/b212204a

[29] Li Y, Rizzo A, Salerno M, Mazzeo M, Huo C, Wang Y, et al. Multifunctional platinum porphyrin dendrimers as emitters in undoped phosphorescent based light emitting devices. Applied Physics Letters. 2006;**89**:061125(1-3). DOI: 10.1063/1.2335511

[30] Graham KR, Yang Y, Sommer JR, Shelton AH, Schanze KS, Xue J, et al. Extended conjugation platinum(II) porphyrins for use in near-infrared emitting organic light emitting diodes. Chemistry of Materials. 2011;**23**:5305-5312. DOI: 10.1021/cm202242x

[31] Lin YY, Chan SC, Chan MCW, Hou YJ, Zhu N, Che CM, et al. Structural, photophysical, and electrophosphorescent properties of platinum(II) complexes supported by tetradentate N_2O_2 chelates. Chemistry - A European Journal. 2003;**9**:1263-1272. DOI: 10.1002/chem.200390143

[32] Che CM, Chan SC, Xiang HF, Chan MCW, Liu Y, Wang Y. Tetradentate Schiff base platinum(II) complexes as new class of phosphorescent materials for high-efficiency and white-light electroluminescent devices. Chemical Communications. 2004;**40**:1484-1485. DOI: 10.1039/b402318h

[33] Che CM, Kwok CC, Lai SL, Rausch AF, Finkenzeller WJ, Zhu N, et al. Photophysical properties and OLED applications of phosphorescent platinum(II) Schiff base complexes. Chemistry - A European Journal. 2010;**16**:233-247. DOI: 10.1002/chem.200902183

[34] Zhou L, Kwong CL, Kwok CC, Cheng G, Zhang H, Che CM. Efficient red electroluminescent devices with sterically hindered phosphorescent platinum(II) Schiff base complexes and iridium complex codopant. Chemistry - An Asian Journal. 2014;**9**:2984-2994. DOI: 10.1002/asia.201402618

[35] Chi Y, Chou PT. Transition-metal phosphors with cyclometalating ligands: Fundamentals and applications. Chemical Society Reviews. 2010;**39**:638-655. DOI: 10.1039/b916237b

[36] Kui SCF, Chow PK, Tong GSM, Lai SL, Cheng G, Kwok CC, et al. Robust phosphorescent platinum(II) complexes containing tetradentate O^N^C^N ligands: Excimeric excited state and application in organic white-light-emitting diodes. Chemistry - A European Journal. 2013;**19**:69-73. DOI: 10.1002/chem.201203687

[37] Lai SL, Tong WY, Kui SCF, Chan MY, Kwok CC, Che CM. High efficiency white organic light-emitting devices incorporating yellow phosphorescent platinum(II) complex and composite blue host. Advanced Functional Materials. 2013;**23**:5168-5176. DOI: 10.1002/adfm.201300281

[38] Kui SCF, Chow PK, Cheng G, Kwok CC, Kwong CL, Low KH, et al. Robust phosphorescent platinum(II) complexes with tetradentate O^N^C^N ligands: High efficiency OLEDs with excellent efficiency stability. Chemical Communications. 2012;**49**:1497-1499. DOI: 10.1039/c2cc37862k

[39] Cheng G, Kui SCF, Ang WH, Ko MY, Chow PK, Kwong CL, et al. Structurally robust phosphorescent [Pt(O^N^C^N)] emitters for high performance organic light-emitting devices with power efficiency up to 126 lm w^{-1} and external quantum efficiency over 20%. Chemical Science. 2014;**5**:4819-4830. DOI: 10.1039/c4sc01105h

[40] Cheng G, Wan Q, Ang WH, Kwong CL, To WP, Chow PK, et al.

High-performance deep-red/near-infrared OLEDs with tetradentate [Pt(O^N^C^N)] emitters. Advanced Optical Materials. 2019;**7**:1801452(1-7). DOI: 10.1002/adom.201801452

[41] Cheng G, Chow PK, Kui SCF, Kowk CC, Che CM. High-efficiency polymer light-emitting devices with robust phosphorescent platinum(II) emitters containing tetradentate dianionic O^N^C^N ligands. Advanced Materials. 2013;**25**:6765-6770. DOI: 10.1002/adma.201302408

[42] Hang XC, Fleetham T, Turner E, Brooks J, Li J. Highly efficient blue-emitting cyclometalated platinum(II) complexes by judicious molecular design. Angewandte Chemie International Edition. 2013;**52**:6753-6756. DOI: 10.1002/anie.201302541

[43] Fleetham TB, Huang L, Klimes K, Brooks J, Li J. Tetradentate Pt(II) complexes with 6-membered chelate rings: A new route for stable and efficient blue OLEDs. Chemistry of Materials. 2016;**28**:3276-3282. DOI: 10.1021/acs.chemmater.5b04957

[44] Fleetham T, Li G, Li J. Efficient red-emitting platinum complex with long operational stability. ACS Applied Materials & Interfaces. 2015;**7**:16240-16246. DOI: 10.1021/acsami.5b01596

[45] Li G, Klimes K, Fleetham T, Zhu ZQ, Li J. Stable and efficient sky-blue organic light emitting diodes employing a tetradentate platinum complex. Applied Physics Letters. 2017;**110**:11301(1-5). DOI: 10.1063/1.4978674

[46] Li G, Fleetham T, Turner E, Hang XC, Li J. Highly efficient and stable narrow-band phosphorescent emitters for OLED applications. Advanced Optical Materials. 2015;**3**:390-397. DOI: 10.1002/adom.201400341

[47] Fleetham T, Li G, Li J. Phosphorescent Pt(II) and Pd(II) complexes for efficient, high-color-quality, and stable OLEDs. Advanced Materials. 2017;**29**:1601861. DOI: 10.1002/adma.201601861

[48] Li G, Wolfe A, Brooks J, Zhu ZQ, Li J. Modifying emission spectral bandwidth of phosphorescent platinum(II) complexes through synthetic control. Inorganic Chemistry. 2017;**56**:8244-8256. DOI: 10.1021/acs.inorgchem.7b00961